Available online at www.eccomasproceedia.org
Eccomas Proceedia UNCECOMP (2023) 707-719

ECCOMAS
Proceedia

UNCECOMP 2023
5th ECCOMAS Thematic Conference on
Uncertainty Quantification in Computational Science and Engineering
M. Papadrakakis, V. Papadopoulos, G. Stefanou (eds.)
Athens, Greece, 12-14 June 2023

FLUID-STRUCTURE INTERACTIONS IN STRUCTURAL UPDATING: A SIMPLIFIED APPROACH FOR LTI SYSTEMS

Quentin Dollon[1]

[1]Research Institute of Hydro-Québec (IREQ)
1800 Bd Lionel-Boulet, Varennes, Québec, Canada J3X 1S1
e-mail: dollon.quentin2@hydroquebec.com

Abstract. *This paper describes an extension of a recently published algorithm for structural model updating. The existing method infers uncertain parameters in a finite element model by using modal data from the real asset. The method described in this paper extends this approach to systems subject to fluid-structure interactions. With a linear approximation of fluid-structure interactions, fluid coupling results in added mass and damping in each modal direction, and these quantities become additional parameters to identify. Simulation results showed very good agreement between ground-truth values and identification results even when observations were scarce (less than* 10% *of observed degrees of freedom).*

Keywords: Structural model updating, fluid-structure interaction, Bayesian statistics

ISSN:2623-3339
Peer-review under responsibility of the organizing committee of UNCECOMP 2023.
doi: 10.7712/120223.10369.19925

1 INTRODUCTION

Structural model updating (SMU) is a powerful framework allowing continuous updating of a finite element model (FEM) so that its predictions match real observations. Starting from an FEM with uncertain parameters, a data assimilation routine is implemented to refine parameter certainty. Bayesian data assimilation techniques are particularly suited to SMU as they quantify not only experimental uncertainty but also model uncertainties due to inaccuracies in mathematical foundations. Bayesian-based SMU approaches use a Bayesian scheme that unfolds relevant information about the parameters from the likelihood function. Parameter identification eventually returns the so-called posterior distribution whose probability gives a measure of plausibility for the parameters having a certain value given the data.

In engineering, a wide variety of structures are immersed in water: subsea pipelines, hydropower turbines and ship propellers, to name a few. Such structures are subject to fluid-structure interactions (FSI), that is, complex non-linear interactions between the underwater system and the surrounding flow. Solving the FSI problem generally involves multiple approximations to obtain a reduced order model, resulting in added mass, damping and stiffness parameters.

A Bayesian-based SMU algorithm called APerCEM (augmented perturbed condensed Eigen model) was published recently. This novel algorithm uses a two-stage condensation technique on the finite element Eigen models of a linear time-invariant (LTI) system that allows expression of unobserved degrees of freedom as linear combinations of observed ones while remaining linear in the parameters. The linear characteristics of the model order reduction scheme mean that a Gibbs sampler can be deployed to solve the problem efficiently. The method developed enforces identifiability through model order reduction and allows optimal tracking of the problem through Gibbs sampling.

Our study extends the APerCEM to track FEM parameters of a partially submerged structure using spatially sparse measured degrees of freedom. The model formulation is well suited to incorporation of added parameters as it relies on Eigen models. Focus was made on a hydroelectric turbine whose runner is under water and subject to FSI. Each observed mode was associated with a set of added parameters inferred in a mode-specific way. The rest of the FEM parameters were inferred conditional on FSI and observed modes. Two simulation cases were considered: first, an attempt was made to recover added mass and damping parameters for each of the modes assuming full knowledge of the FEM; next, we assumed partial knowledge of the model and tried to recover the joint distribution of FSI parameters and unknown FEM parameters.

2 FLUID-STRUCTURE INTERACTIONS IN FEM

Fluid-structure interactions describe the relationship between a fluid and a structure submerged in it or exposed to it. When not interacting, the two domains have independent dynamics. The structural domain can be modelled by an FEM governing the displacement field:

$$\boldsymbol{M}_S\ddot{\boldsymbol{u}} + \boldsymbol{C}_S\dot{\boldsymbol{u}} + \boldsymbol{K}_S\boldsymbol{u} = \boldsymbol{F}_S(t) \tag{1}$$

Fluid dynamics are generally complex and derive from the mass and momentum conservation principles expressed in the Navier-Stokes equations. When one is interested only in a local formulation of fluid behavior, to study the propagation of a small per-

turbation for instance, the Laplace or Helmhotz (incompressible fluid) equations can be used. These equations define a d'Alembert operator on the pressure field. This approach is called acoustic and allows one to model the pressure field in the form of an equivalent FEM [1, 2]:

$$\boldsymbol{M}_F\ddot{\boldsymbol{p}} + \boldsymbol{C}_F\dot{\boldsymbol{p}} + \boldsymbol{K}_F\boldsymbol{p} = \boldsymbol{F}_F(t) \tag{2}$$

Note that $\boldsymbol{M}_F, \boldsymbol{C}_F$ and $\boldsymbol{K}_F$ are not conventional mass, damping and stiffness matrices but rather equivalent quantities for pressure fields. When the fluid domain influences the structural domain or vice versa the systems become coupled and the resultant dynamics can be complex, making analysis and prediction of system behavior difficult if not impossible. To simplify the understanding of fluid-structure interactions, a linear approximation for small perturbations was made. This results in a coupling matrix $\boldsymbol{R}$ which allows the fluid-structure system to be modeled as a single FEM [2]:

$$\begin{pmatrix} \boldsymbol{M}_S & \boldsymbol{0} \\ \rho_F\boldsymbol{R}^T & \boldsymbol{M}_F \end{pmatrix} \begin{pmatrix} \ddot{\boldsymbol{u}} \\ \ddot{\boldsymbol{p}} \end{pmatrix} + \begin{pmatrix} \boldsymbol{C}_S & \boldsymbol{0} \\ \boldsymbol{0} & \boldsymbol{C}_F \end{pmatrix} \begin{pmatrix} \dot{\boldsymbol{u}} \\ \dot{\boldsymbol{p}} \end{pmatrix} + \begin{pmatrix} \boldsymbol{K}_S & -\boldsymbol{R} \\ \boldsymbol{0} & \boldsymbol{K}_F \end{pmatrix} \begin{pmatrix} \boldsymbol{u} \\ \boldsymbol{p} \end{pmatrix} = \begin{pmatrix} \boldsymbol{F}_S \\ \boldsymbol{F}_F \end{pmatrix}(t) \tag{3}$$

Study of the modal decomposition of this coupled system indicates that both natural frequencies and damping ratios are affected (generally, mode shapes are affected to a much lesser extent). One simple approach for taking these alterations into account is to define the concepts of added mass and added damping.

Added mass refers to the effective increase in mass of a structure due to the surrounding fluid inertia in a given modal direction. This reflects the fact that a stronger force is needed to move the structure in water than in air. Added damping refers to the equivalent damping introduced by fluid on structure motion. When moving into water, the structure imparts a fraction of its energy to the fluid. Added damping models this transfer process as an equivalent damping effect on the structure. By using added mass and added damping, a simpler and more manageable linear model of the fluid-structure system can be obtained, making it easier to analyze and predict its behavior. These added parameters are mode-specific, that is, there is a single pair of added damping and added mass parameters per mode.

3 PHYSICAL MODELLING

Structural model updating using modal characteristics has gathered much attention over the last decade (see, for instance, [3, 4, 5] and related references). This comes from the need for structural parameter fine-tuning in FEMs. Indeed, despite the increasing sophistication of FEMs, predictions still often show major discrepancies from experimental results. This can be due, among other reasons, to a poor choice of physical parameters in the model [6]. SMU is a branch of inverse problems dedicated to calibrating FEM parameters using real data. Instead of running simulations and comparing them to data, observations are used as input to infer the parameters.

PerCEM is a class of forward models used to update FEMs based on spatially scarce modal observations (that is, modes of the structure are observed on a very restricted number of degrees of freedoms). PerCEM was recently introduced in other papers by the author [5]. The acronym stands for Perturbed Condensed Eigen model. An overview of the method that does not take FSI into consideration is described below. the model is then modified to take into account added mass and damping.

3.1 PerCEM formulation

The classic FEM formulation is divided into two parts, a deterministic part with known parameters and an uncertain part with unknown parameters.

$$[\boldsymbol{M}_0 + \boldsymbol{M}(\boldsymbol{\vartheta})]\,\ddot{\boldsymbol{u}} + [\boldsymbol{C}_0 + \boldsymbol{C}(\boldsymbol{\vartheta})]\,\dot{\boldsymbol{u}} + [\boldsymbol{K}_0 + \boldsymbol{K}(\boldsymbol{\vartheta})]\,\boldsymbol{u} = \boldsymbol{F}_S(t) \tag{4}$$

The uncertain parameters $\boldsymbol{\vartheta}$ are unknown mass, damping and stiffness coefficients. The goal of identification is to provide estimates for these coefficients. It all starts with the Eigen models of (4). For any mode with pole λ_n and shape $\boldsymbol{a}_n$, one has:

$$\boldsymbol{Z}(\lambda_n, \boldsymbol{\vartheta})\boldsymbol{a}_n = \boldsymbol{\varepsilon}_n \tag{5}$$

where $\boldsymbol{Z}(\lambda_n, \boldsymbol{\vartheta})$ is the nth modal pencil matrix:

$$\boldsymbol{Z}(\lambda_n, \boldsymbol{\vartheta}) = \lambda_n^2\,[\boldsymbol{M}_0 + \boldsymbol{M}(\boldsymbol{\vartheta})] + \lambda_n\,[\boldsymbol{C}_0 + \boldsymbol{C}(\boldsymbol{\vartheta})] + [\boldsymbol{K}_0 + \boldsymbol{K}(\boldsymbol{\vartheta})] \tag{6}$$

It is often stated that model (5) equals zero. In reality, the formulation always deviates slightly from zero because numerical solutions are never exact. This is not a problem if Eigen models are used directly. However, if linear algebra is used to manipulate the model, ill-conditioning issues can occur. This is why a small perturbation term ε_n is introduced. Eigen model formulations suffer from a major drawback: they consider that mode shapes are known for all nodes in all directions. In practice, this knowledge is often sparse, and shapes are only known in a few node directions. In order to make expression (5) dependent only on the partially observed shape $\boldsymbol{\psi}_n$, a condensation technique is used to obtain:

$$\boldsymbol{R}(\lambda_n, \boldsymbol{\vartheta})\boldsymbol{\psi}_n + \boldsymbol{T}(\lambda_n, \boldsymbol{\vartheta})\boldsymbol{\varepsilon}_n = \boldsymbol{0} \tag{7}$$

This last expression is the perturbed condensed Eigen model (PerCEM). The term $\boldsymbol{T}(\lambda_n, \boldsymbol{\vartheta})\boldsymbol{\varepsilon}_n$ is necessary because the condensation introduces ill-conditioning. Then, even if $\boldsymbol{\varepsilon}_n$ is a negligible term, $\boldsymbol{T}(\lambda_n, \boldsymbol{\vartheta})\boldsymbol{\varepsilon}_n$ is not. For more details on deriving $\boldsymbol{R}(\lambda_n, \boldsymbol{\vartheta})$ and $\boldsymbol{T}(\lambda_n, \boldsymbol{\vartheta})$ from $\boldsymbol{Z}(\lambda_n, \boldsymbol{\vartheta})$, refer to [5].

3.2 FSI modelling

As mentioned previously, FSI can be introduced with the help of added parameters. Here, an added mass and added damping are assumed to exist for each mode, but this can easily be extended to added stiffness as well. We considered the case of a partially submerged structure. Each mode has a local added mass m_n and added damping c_n applied on nodes immersed in water. These parameters are gathered in a vector $\boldsymbol{\eta}_n$. The Eigen model (5) then becomes:

$$\boldsymbol{Z}(\lambda_n, \boldsymbol{\vartheta}, \boldsymbol{\eta}_n)\boldsymbol{a}_n = \boldsymbol{\varepsilon}_n \tag{8}$$

Where:

$$\boldsymbol{Z}(\lambda_n, \boldsymbol{\vartheta}, \boldsymbol{\eta}_n) = \lambda_n^2\,[\boldsymbol{M}_0 + \boldsymbol{M}(\boldsymbol{\vartheta}) + \boldsymbol{M}_n(\boldsymbol{\eta}_n)] + \lambda_n\,[\boldsymbol{C}_0 + \boldsymbol{C}(\boldsymbol{\vartheta}) + \boldsymbol{C}_n(\boldsymbol{\eta}_n)] + [\boldsymbol{K}_0 + \boldsymbol{K}(\boldsymbol{\vartheta})] \tag{9}$$

Matrices $\boldsymbol{M}_n(\boldsymbol{\eta}_n)$ and $\boldsymbol{C}_n(\boldsymbol{\eta}_n)$ are zero everywhere except on immersed degrees of freedom subject. If there are n_{FSI} of such degrees of freedom, then the interaction term

is m_n/n_{FSI} and c_n/n_{FSI}. In this way, the contribution of added parameters is shared between all the immersed degrees of freedom. The nth PerCEM is given by:

$$\boldsymbol{R}(\lambda_n, \boldsymbol{\vartheta}, \boldsymbol{\eta}_n)\boldsymbol{\psi}_n + \boldsymbol{T}(\lambda_n, \boldsymbol{\vartheta}, \boldsymbol{\eta}_n)\boldsymbol{\varepsilon}_n = \mathbf{0} \tag{10}$$

The technique used to condense the model is the same as in the original formulation except that the parametrized manifold includes the FSI-influenced degrees of freedom [5]. The model order reduction scheme relies on a two-stage procedure that preserves linearity. Hence, matrices $\boldsymbol{R}(\lambda_n, \boldsymbol{\vartheta}, \boldsymbol{\eta}_n)$ and $\boldsymbol{T}(\lambda_n, \boldsymbol{\vartheta}, \boldsymbol{\eta}_n)$ are linear with respect to $\boldsymbol{\vartheta}$ and $\boldsymbol{\eta}_n$.

4 INFERENCE

Once the model was obtained, a statistical procedure was implemented to identify the model. First, the observed data had to be accounted for in the physical model, and then the parameters of interest needed to be inferred.

Equations (8) and (10) are complex valued. This is because modal poles are complex and the shape can also be complex (for instance in the presence of gyroscopic effects). Unless quantities are circular symmetric, that is, their probability density function is phase-invariant on the complex plane, it can be difficult to handle complex values in statistics. In order to work with real-valued models, the real and imaginary parts were separated and treated independently. This led to augmentation of the perturbed condensed Eigen model (APerCEM),

$$\boldsymbol{R}^\star(\lambda_n, \boldsymbol{\vartheta}, \boldsymbol{\eta}_n)\boldsymbol{\psi}_n^\star + \boldsymbol{T}^\star(\lambda_n, \boldsymbol{\vartheta}, \boldsymbol{\eta}_n)\boldsymbol{\varepsilon}_n^\star = \mathbf{0} \tag{11}$$

The augmented matrices and vectors are given by:

$$\boldsymbol{A}^\star = \begin{pmatrix} \Re(\boldsymbol{A}) & -\Im(\boldsymbol{A}) \\ \Im(\boldsymbol{A}) & \Re(\boldsymbol{A}) \end{pmatrix}, \quad \boldsymbol{a}^\star = \begin{pmatrix} \Re(\boldsymbol{a}) \\ \Im(\boldsymbol{a}) \end{pmatrix} \tag{12}$$

4.1 Statistical model

Assume that a set of I modes was characterized from the measured data. For each mode, J samples were available for pole and shape, giving a dataset $\boldsymbol{\mathcal{D}}_i = \left\{\hat{\lambda}_{ij}, \hat{\boldsymbol{\psi}}_{ij}; 1 \leq j \leq J\right\}$. The statistical model aims to connect observations to the model through a probability density function. These distributions are chosen Gaussian according to maximum entropy theory [7]. For mode shapes,

$$\hat{\boldsymbol{\psi}}_{ij}^\star \sim \mathcal{N}\left(\boldsymbol{\psi}_i^\star, \boldsymbol{\Sigma}_i\right) \tag{13}$$

Where $\boldsymbol{\Sigma}_i$ is a diagonal matrix, whose entries correspond to the variance of real and imaginary parts of the partial mode shape samples. Parameters $\boldsymbol{\varepsilon}_i$ are considered centred with a given prior variance σ^2 (which is independent of i):

$$\boldsymbol{\varepsilon}_i^\star \sim \mathcal{N}\left(\mathbf{0}, \sigma^2 \boldsymbol{I}\right) \tag{14}$$

Observed poles are used in the APerCEM to give the following experimental evaluation:

$$\boldsymbol{R}^\star(\hat{\lambda}_{ij}, \boldsymbol{\vartheta}, \boldsymbol{\eta}_i)\boldsymbol{\psi}_i^\star + \boldsymbol{T}^\star(\hat{\lambda}_{ij}, \boldsymbol{\vartheta}, \boldsymbol{\eta}_i)\boldsymbol{\varepsilon}_i^\star \sim \mathcal{N}\left(\mathbf{0}, \boldsymbol{\Delta}_i\right) \tag{15}$$

Covariance matrices $\boldsymbol{\Delta}_i$ are diagonal with unknown entries, and represent the variance of the real and imaginary parts of the APerCEM realizations.

At step n**,**

Sample $\boldsymbol{\vartheta}^{(n)}|\{\boldsymbol{\eta}_i^{(n-1)}, \boldsymbol{\psi}_i^{(n-1)}, \boldsymbol{\varepsilon}_i^{(n-1)}, \boldsymbol{\Delta}_i^{(n-1)}\}_i, \boldsymbol{\mathcal{D}}$

For all i:

Sample $\boldsymbol{\eta}_i^{(n)}|\boldsymbol{\vartheta}^{(n)}, \boldsymbol{\psi}_i^{(n-1)}, \boldsymbol{\varepsilon}^{(n-1)}, \boldsymbol{\Delta}_i^{(n-1)}, \boldsymbol{\mathcal{D}}_i$

Construct sampled PerCEM matrices $\boldsymbol{R}(\hat{\lambda}_{ij}, \boldsymbol{\vartheta}^{(n)}, \boldsymbol{\eta}_i^{(n)})$ and $\boldsymbol{T}(\hat{\lambda}_{ij}, \boldsymbol{\vartheta}^{(n)}, \boldsymbol{\eta}_i^{(n)})$

Sample $\boldsymbol{\psi}_i^{(n)}|\boldsymbol{\vartheta}^{(n)}, \boldsymbol{\eta}_i^{(n)}, \boldsymbol{\varepsilon}_i^{(n-1)}, \boldsymbol{\Delta}_i^{(n-1)}, \boldsymbol{\mathcal{D}}_i$

Sample $\boldsymbol{\varepsilon}_i^{(n)}|\boldsymbol{\vartheta}^{(n)}, \boldsymbol{\eta}_i^{(n)}, \boldsymbol{\psi}_i^{(n)}, \boldsymbol{\Delta}_i^{(n-1)}, \boldsymbol{\mathcal{D}}_i$

Construct sampled APerCEM samples $\boldsymbol{R}(\hat{\lambda}_{ij}, \boldsymbol{\vartheta}^{(n)}, \boldsymbol{\eta}_i^{(n)})\boldsymbol{\psi}_i^{(n)} + \boldsymbol{T}(\hat{\lambda}_{ij}, \boldsymbol{\vartheta}^{(n)}, \boldsymbol{\eta}_i^{(n)})\boldsymbol{\varepsilon}_i^{(n)}$

Sample $\boldsymbol{\Delta}_i^{(n)}|\boldsymbol{\vartheta}^{(n)}, \boldsymbol{\eta}_i^{(n)}, \boldsymbol{\psi}_i^{(n)}, \boldsymbol{\varepsilon}_i^{(n)}, \boldsymbol{\mathcal{D}}_i$

Table 1: Gibbs sampling algorithm

4.2 Gibbs sampling

The parameters in the statistical model that need to be identified are the FEM parameters $\boldsymbol{\vartheta}$, the FSI added parameters $\boldsymbol{\eta}_i$, the mode shapes $\boldsymbol{\psi}_i$, the perturbations $\boldsymbol{\varepsilon}_i$ and the APerCEM covariance matrices $\boldsymbol{\Delta}_i$, with $1 \leq i \leq I$. The information about these parameters is carried by functions (13) and (15), the so-called likelihood functions. Bayesian theory is used to extract this information. This statistical framework makes it possible to characterize the distribution of unknown parameters conditional on data using likelihood functions and prior knowledge about the parameters. The prior is similar to regularization in optimization problems. In our model, prior (14) is given to perturbations so values of $\boldsymbol{\varepsilon}_i$ will not become too large during identification.

A Gibbs sampler is used to solve the Bayesian problem. Gibbs sampling is a Markov chain Monte Carlo (MCMC) method used for exploring the probability space of unknown parameters in the Bayesian model. The method involves updating one parameter at a time based on the current value of other parameters. This is done by successive sampling from the conditional distribution of each parameter, making it easier to converge to the target distribution. Gibbs samplers also have the advantage of being easy to implement and computationally efficient. In our model, we have Gaussian likelihoods and linearity with respect to the parameters; hence conditional distributions are easy to derive and take the form of Gaussian distributions. The variance parameters have Inverse Gamma kernel distributions. Table 1 shows the general algorithm for implementing a Gibbs sampler on AperCEM models.

5 SIMULATION STUDY

5.1 Test case definition

For this project, we updated the structural model of a hydroelectric generating unit inspired by an actual prototype. The generating unit is composed of a runner, a generator, a thrust bearing and two tilting-pad hydrodynamic guide bearings, the upper guide bearing (UGB) and the lower guide Bearing (LGB). The different subcomponents are connected through a hollow shaft in a vertical position rotating at a synchronous speed of 134 rpm.

The hydroelectric generating unit was discretized using 29 nodes as shown in Figure 1. Node locations were chosen to account for rotor subcomponents and changes in geometry. Each node has two transverse displacement coordinates and two rotation coordinates.

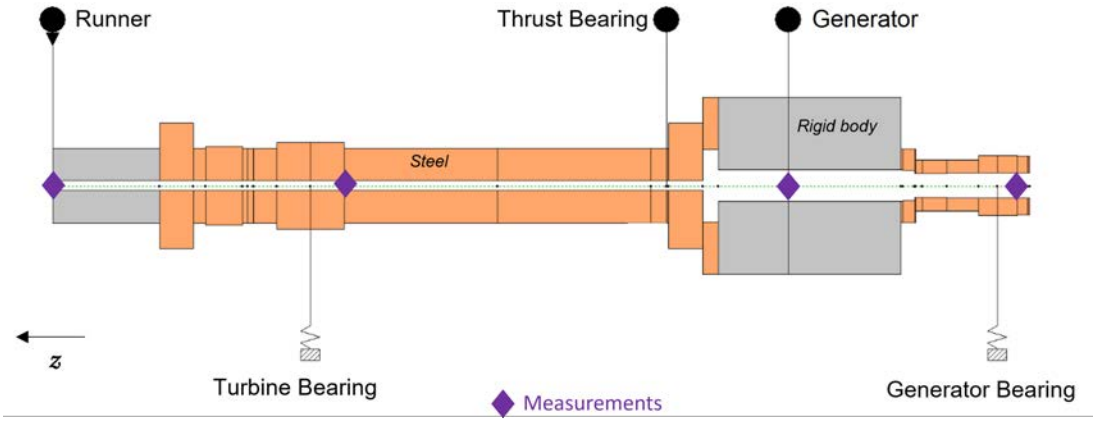

Figure 1: Rotor geometry used in the FEM

The one-dimensional FEM then has 116 degrees of freedom and is constructed using rotordynamic theory [8]. It is designed for lateral vibration analysis. Timoshenko shaft elements were used to account for a rotational bending mechanism and shear deformation. The thrust bearing induces both rotational stiffness and damping [9]. Guide bearings are supposed to behave linearly and were characterized by four stiffness and four damping coefficients. The runner, generator and thrust bearing block were modelled using rigid disks of given mass, polar and diametral moments of inertia. The runner is immersed in water and subject to FSI.

The system was virtually monitored by four pairs of proximeter sensors recording transverse displacements at runner seals (x1), bearing housings (x2) and the rotor-stator air gap in the generator (x1). This instrumentation is a good representation of what might be found in a real asset monitoring system. Hence, 7% of the FEM degrees of freedom were observed. The procedure used to produce synthetic modal data is illustrated in Figure 2. An uncalibrated and FSI-free FEM was considered first. Ground-truth values were chosen for both the physical parameters and the added parameters. A calibrated FEM was obtained using the physical parameters. As each mode is subject to a different FSI, the calibrated FEM was successively altered with different pairs of added parameters. From each of these modified FEMs, one mode was extracted and used to construct the synthetic dataset. Noise was then introduced and a set of $J = 100$ samples was drawn to produce the input data. In the case studies discussed below, $I = 15$ modes were taken to construct the input.

Two cases were investigated. In a first scenario, the FEM was assumed perfectly known with unknown FSI. The purpose here was to recover underlying added parameters for each mode, giving 30 parameters to identify. Next, an uncertain FEM was considered subject to unknown FSI. Both FEM parameters and added parameters had to be recovered. It was decided that the guide-bearing damping and stiffness parameters would need to be updated in the model, leaving 16 physical parameters to be inferred along with the 30 added parameters. Table 2 shows the ground-truth parameters. Bearing characteristics were obtained using hydrodynamic short-bearing theory [10]. Added parameters were picked randomly with some constraints. Added masses were chosen in the same order of magnitude as the runner mass (weight = 85 tons). Added damping values were chosen so that added modal damping ratios lay between 0% and 5%. For modes 2 and 3, positive added damping resulted in negative added damping ratios, meaning modal response

Upper Guide bearing (UGB)							
k_{xx}^U	6.51e8	k_{xy}^U	-7.86e7	c_{xx}^U	3.71e7	c_{xy}^U	-4.80e7
k_{yx}^U	-1.54e9	k_{yy}^U	1.99e9	c_{yx}^U	-4.80e7	c_{yy}^U	1.72e8
Lower Guide Bearing (LGB)							
k_{xx}^L	1.10e8	k_{xy}^L	1.07e10	c_{xx}^L	1.53e9	c_{xy}^L	-7.84e6
k_{yx}^L	-1.07e10	k_{yy}^L	5e47e7	c_{yx}^L	-7.84e6	c_{yy}^L	1.53e9

Modal Added Parameters				
Mode i	Added mass m_i	Added damping c_i	FRR	α_{add}[%]
1	1.00e5	7.52e7	0.93	2.00
2	9.83e4	1.26e7	0.98	-0.3
3	7.80e4	9.99e5	0.93	-2.48
4	6.09e4	7.92e6	0.94	9.50
5	7.00e4	1.01e7	1	5.10
6	5.08e4	1.43e6	0.91	1.29
7	5.09e4	6.45e6	0.92	4.81
8	7.05e4	1.65e6	1	1.04
9	3.48e4	2.90e6	0.96	0.26
10	4.87e4	1.64e7	0.96	0.97
11	6.67e4	1.20e7	0.99	0
12	7.49e4	1.92e6	0.99	0
13	5.15e4	1.51e8	1	0
14	3.07e4	7.32e7	1	0
15	5.15e4	1.37e8	1	0

Table 2: Ground-truth parameter values: mass in kg, stiffness in N/m and damping in Ns/m

instabilities can be induced from FSI. Table 2 also includes FRRs (Frequency Reduction Ratio) and added damping ratios, common quantities in engineering. FRR is the ratio of natural frequencies in water and in air and represents the decrease in natural frequencies when FSI are considered. The added damping ratio α_{add} represents the change in damping ratio due to FSI. The added damping ratio and FRR need modal references to be computed. These references correspond to the modes of the FEM without FSI. Modal pairing between FSI-free FEM and FEMs with FSI was based on the modal assurance criterion (MAC) [11]. Mode shapes are generally barely influenced by FSI, and obtained MACs for modes in air and modes in water were between 89.6% and 99.9%.

5.2 Identification results

A Markov chain of 500 samples was constructed. Initialization was set to zero for all parameters. Flat priors were chosen so as to not bias the results and to assess model sensitivity to data. A 5% coefficient of variation was imposed on made shapes, while poles had a variance of 1.58 rad^2 and 1.1 rad^2 for real and imaginary parts, respectively. The initial sequences of the chain were disregarded as they take place during the transient period where the chain converges toward the posterior distribution. This burn-in was very fast, however, and took less than 10 iterations. Results for FSI identification and for dual FSI-parameter identification are presented in Figures 3 to 5.

Figures 3 and 4 show results for added parameters when the FEM is known and when it is uncertain, respectively. Joint distribution of added mass and damping is presented

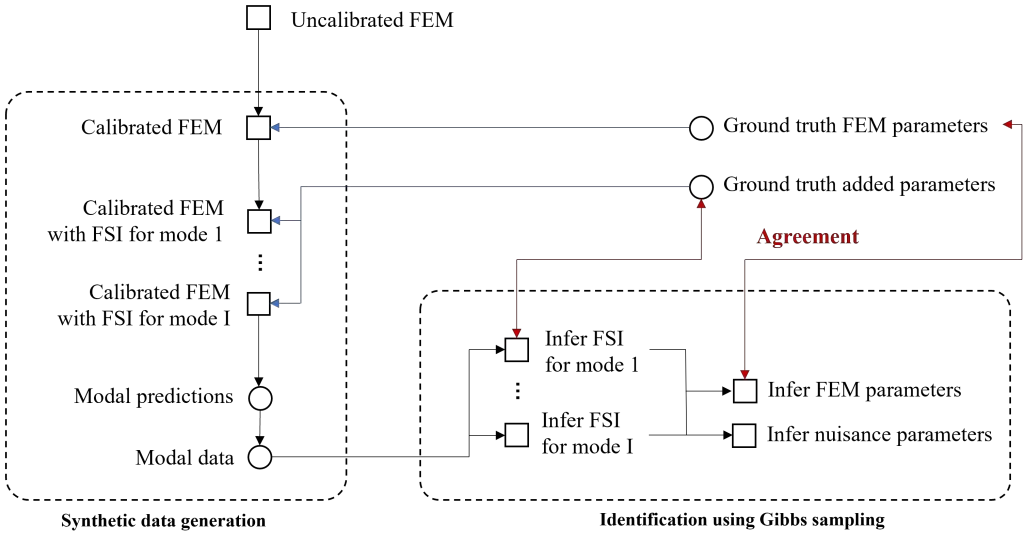

Figure 2: Procedure for validation using synthetic data

as well as the ground truth reference plot (in red). The posterior distributions are very similar in both cases. They accurately recover ground truth for most modes, indicating that the accuracy of FSI identification is only marginally influenced by knowledge in the FEM. This, of course, only holds when parameter locations are exactly specified in the physical model class.

FSI seemed to have a weak impact on mode 2, making it difficult to restore them from observations. While added mass is sampled around zero, added damping samples go from 0 Ns/m to $1e7$ Nm/s, leading to a significant under-estimation. However, when the FEM is also updated, extra variability seems to push Markov chains toward more reasonable solutions, as shown in Figure 5.

Posteriors globally suggest the added parameter samples were independent except for modes 13 and 14, where a slight linear correlation appears. Point estimates of the parameters were obtained using posterior mode, that is, maximum a-posteriori (MAP). MAPs proved accurate compared to ground-truth with an averaged error of 1% for added mass and 3% for added damping except for modes 1 and 2, where errors were drastically higher (50% and 100% for added mass, and 5% and 82% for added damping). If mode 2 is excluded, posterior variances are a good indicator of identification precision, giving reliable confidence intervals.

Figure 5 presents the inference for the FEM bearing parameters. The top row shows the UGB results and the bottom row the LGB results. MAP estimates are very close to their ground-truth values. Highest errors occured for LGB cross-damping coefficients, with 20% and 52% errors for c^L_{xy} and c^L_{yx}, respectively. However, uncertainties were also high, and z-scores remained below 3, which is acceptable. Ignoring these two parameters, relative errors are in the order of 1%. Note as well that posterior variance for both LGB cross-stiffness and cross-damping is not wide enough to provide a reliable uncertainty quantification and gives z-scores lower than 3.

6 CONCLUSIONS

This paper describes a first attempt to enrich numerical models of fluid-structure systems with data in order to refine simulation predictions. It is based on enhancement of

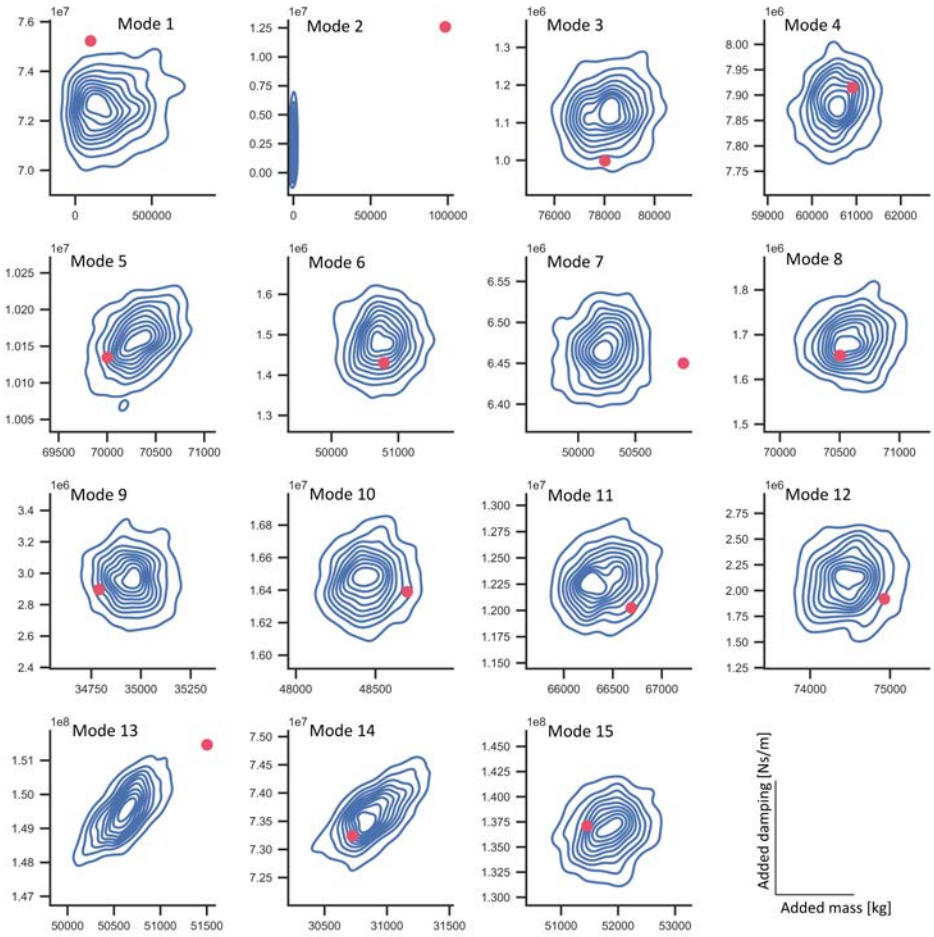

Figure 3: Added parameter identification results conditional on a perfectly known FEM

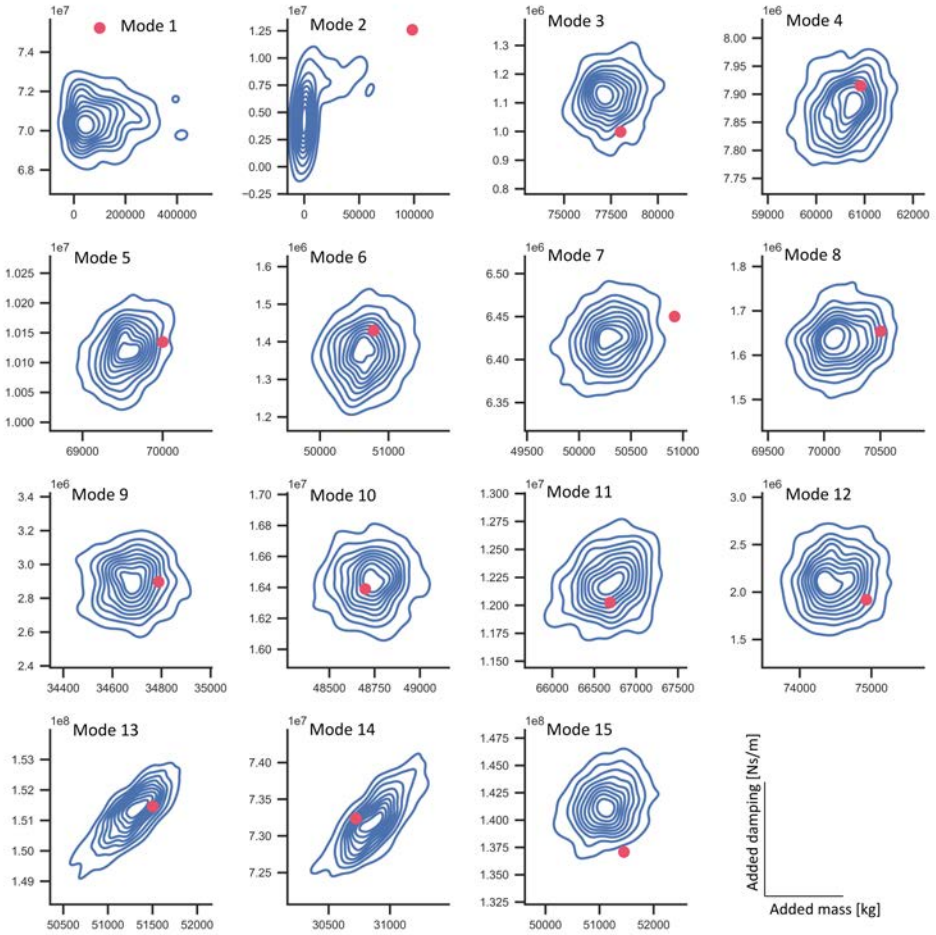

Figure 4: Added parameter identification results conditional on an uncertain FEM

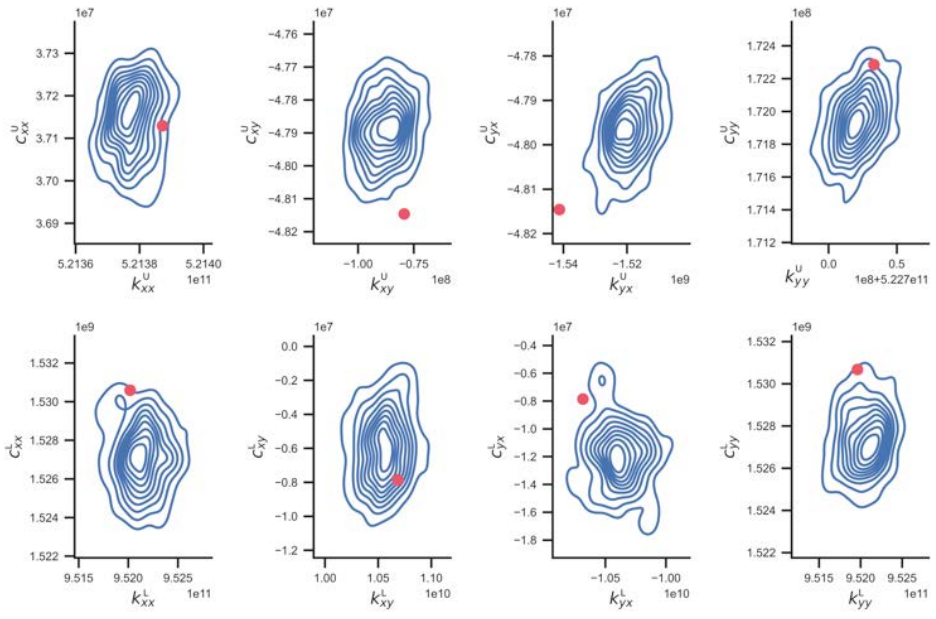

Figure 5: FEM parameter identification results

an existing approach and relies on modal observations to calibrate FEMs. The simulation study delivered promising results and there is good reason to hope the approach can be deployed on actual data.

The major limitation of this work is the use of linear behavior for FSI, which can be unrealistic in a number of cases. In some situations, viscous damping approximations may not accurately represent added damping. For example, in turbines that operate in complex flow regimes (part load and no-load), other types of damping mechanisms such as turbulence-induced and vortex-induced vibrations may play a significant role in FSI, and more sophisticated models must be used to better reflect the added damping.

Moreover, modal approaches become meaningless when non-linearities occur, and accounting for FSI in the non-linear FEM becomes a significant problem that must be solved in the time domain. Future studies will focus on this, in particular on constructing reduced order models of non-linear dynamics and improving predictions capabilities using data.

REFERENCES

[1] A.S. Dehkharqani, J.O. Aidanpaa, F. Engstrom, M.J. Cervantes, A Review of Available Methods for the Assessment of Fluid Added Mass, Damping, and Stiffness With an Emphasis on Hydraulic Turbines. *Applied Mechanics Reviews volume 70-5*, 2018.

[2] C.G. Rodriguez, P. Flores, F.G. Pierart, L.R. Contentz, E. Egusquiza, Capability of structural–acoustical FSI numerical model to predict natural frequencies of submerged structures with nearby rigid surfaces. *Computers and Fluids volume 64*, 2012.

[3] J. Ching, M. Muto, J. Beck, Structural model updating and health monitoring with incomplete modal data using Gibbs sampler. *Computer-Aided Civil and Infrastructure Engineering volume 21-4*, 2006.

[4] S. Cheung, S. Bansal, A new Gibbs sampling based algorithm for bayesian model updating with incomplete complex modal data. *Mechanical Systems and Signal Processing volume 92*, 2017.

[5] Q. Dollon, Efficient structural model updating with spatially sparse modal data: a Bayesian perspective. *Mechanical Systems and Signal Processing 195*, 2023.

[6] J. Mottershead, M. Link, M, Friswell, The sensitivity method in finite element model updating: a tutorial. *Mechanical Systems and Signal Processing 25*, 2011.

[7] E. Jaynes, Where do we stand on maximum entropy? *Proceedings of the Maximum Entropy Formalism Conference*, MIT, 1978.

[8] M. Friswell, J. Penny, S. Garvey, A. Lees, Dynamics of rotating machines. *Cambridge University Press*, 2010.

[9] S. Cupillard, J.O. Aidanpaa, Influence of the thrust bearing on natural frequencies of a 72MW hydropower rotor. *IOP Conf. Ser.: Earth Environ. Sci. 49 082024*, 2016.

[10] B.J. Hamrock, S.R. Schmid, B.O. Jacobson, Fundamental of fluid film lubrication. *Taylor and Francis*, 2004.

[11] M. Pastor, M. Binda, T. Harcarik, Modal assurance criterion. *Procedia Engineering 48*, 2012.